MIMO Radar with Frequency Diversity

Jun Jason Zhang and Antonia Papandreou-Suppappola
Department of Electrical Engineering, Arizona State University, Tempe, AZ, USA
E-mail: Jun.Zhang.EE@asu.edu, papandreou@asu.edu

***Abstract*— We propose a new multiple-input, multiple-output (MIMO) radar system with colocated antennas that can greatly reduce target fluctuations. This is achieved by employing frequency diversity. The proposed MIMO radar system results in a radar array with frequency-division multiplexing that can also incorporate beamforming to design the transmission beam pattern. After presenting an overview of existing MIMO radar systems and their related signal models, we provide a detailed description of the proposed frequency diversity technique and the corresponding transmitter and receiver structures. Furthermore, we present a maximum likelihood estimation algorithm that incorporates frequency diversity with MIMO radar, derive the corresponding Cramér-Rao lower bound, and demonstrate its improved performance using numerical results.**

I. Introduction

Currently, two types of MIMO radar systems are being investigated: MIMO radars with widely-separated antennas and MIMO radars with colocated antennas. Both have many unique advantages, but both also face many challenges.

MIMO radar with widely-separated antennas have two important features: space-diversity and spatial multiplexing. As a result, they can exploit radar cross section (RCS) diversity [1], they can handle slow moving targets by exploiting Doppler estimates from multiple directions [2], and they can support high resolution target localization [3]. However, they can also face problems with time and phase synchronization. As the data volume to be transmitted to the processing center in real time is very large, these radars also face transmission and processing issues. Also, as they employ isotropic transmission antennas that transmit energy evenly to space [4], they cannot use most of their energy to illuminate the target and thus experience losses in signal-to-noise ratio (SNR).

MIMO radar with colocated antennas can exploit waveform diversity. This is important as it can: (a) significantly improve system identification; (b) increase target detection and parameter estimation performance when combined with adaptive arrays; (c) enhance transmit beam pattern design [5]; and (d) enable the design of airborne or ship-borne radars. However, because the antennas are colocated, the main drawback is the loss of space diversity which is needed to mitigate the effect of target fluctuations.

In this paper, we propose a new MIMO radar system that can exploit frequency diversity. This new system uses colocated antennas but with a unique configuration that can still be used to mitigate the effect of target fluctuations and it can also be used for beam pattern synthesis. The paper is organized as follows. In Section II, we discuss frequency diversity, and we introduce the transmitter and receiver architectures of MIMO radar with frequency diversity in Section III. In Section IV, we develop the CRLB for estimating moving target parameters using the proposed radar system, and we provide some corresponding numerical examples in Section V.

This work was supported in part by the Department of Defense Grant No. AFOSR FA9550-05-1-0443.

II. Frequency Diversity

Frequency diversity is a technique that can significantly reduce target fluctuations and improve radar detection performance under agreeable or adverse weather conditions. This type of diversity is possible because the radar-cross-section (RCS) of a complex target varies with both transmitted frequency and target geometry [6], [7]. Although the behavior of real targets can be quite complex, the change in frequency and angle required to decorrelate a target or clutter can be obtained using the relation

$$\Delta F = \frac{c}{2\,L\sin(\vartheta)}\ ,$$

where c is the speed of electromagnetic waves, L is the length of the target, and ϑ is the aspect angle between the target and the radar boresight. Note that $L\sin(\vartheta)$ is the length of the target projected along the radar boresight. As an example, consider a target that is about 5 m long. At L-band (1 GHz), the frequency step required for decorrelation with an aspect angle of $\pi/4$ is 42.4 MHz. This result does not depend on the transmitted frequency. Although the above result is based on a highly simplified target model, since most targets do not consist of a large collection of linearly distributed scatterers, this frequency step may not completely result in decorrelated returns from a target at all aspects. However, this value should be sufficient to avoid deep fading.

Frequency diversity was successfully used in the design of *frequency agile radar* to force decorrelation of successive measurements. In this case, the radar frequency increased by ΔF Hz or more between successive pulses, ensuring that the target echo decorrelated from one pulse to the next. Experimental results with improved target detectability with frequency-agility transmission were provided in [6]. Note that frequency diversity was also investigated in other radar systems. Specifically, the detection of fluctuating targets with multiple frequency diversity channels was investigated in [8]; and the authors in [9], [10] considered frequency diversity for radars with multiple antennas.

 9781-4244-2971-4/09/$25.00©2009 IEEE

III. MIMO Radar Architectures with Frequency Diversity

A. Transmitter Architecture

The transmitter architecture for a MIMO radar system that can exploit frequency diversity is depicted in Fig. 1. As demonstrated, there are N_T transmission antennas in this design, and each antenna is able to transmit N_F different carrier frequencies at the same time. At the ith transmit antenna, $i = 1, \ldots, N_T$, the mth carrier frequency f_m, $m = 1, \ldots, N_F$, is modulated by the mth transmission signal $s_m(t)$, and weighted by the weighting factor $\alpha_{i,m}$. If we only have one transmission antenna, i.e. $N_T = 1$, the resulting radar architecture is the same as the frequency diversity radar in [8]. Although the system in [8] can achieve frequency diversity, it cannot be used for beamforming and estimation of direction of arrival (DOA). If we only have one transmission frequency, i.e. $N_F = 1$, the resulting architecture is a standard radar phased array that can be used for beamforming and DOA estimation, but cannot be used to mitigate target fluctuation.

The radar transmission signal is described as follows. We denote the steering vector for the signal on the mth carrier frequency as $\mathbf{b}_m(\theta) = [b_m(1,\theta), \cdots, b_m(N_T,\theta)]^{\mathbb{T}}$, whose ith element is $b_m(i,\theta)$. For a uniform linear array (ULA), if the antennas are spaced by distance d, then

$$b_m(i,\theta) = \exp\left(j2\pi\frac{f_m}{c}(\frac{N_T-1}{2} - i)d)\sin(\theta)\right).$$

We also weigh $s_m(t)$ before it is transmitted, and we denote the weight vector by $\boldsymbol{\alpha}_m = [\alpha_{1,m}, \cdots, \alpha_{N_T,m}]^{\mathbb{T}}$, where $\alpha_{i,m}$ is the weight multiplied to $s_m(t)$ on the ith antenna. At the far field, with direction angle θ, the transmission beam pattern for the signal on the mth carrier frequency is defined as

$$B_m(\theta) = \mathbf{b}_m^{\mathbb{T}}(\theta)\boldsymbol{\alpha}_m.$$

We consider a MIMO frequency diversity radar with a uniform linear array with N_T antennas. The N_F carrier frequencies are chosen as $f_m = f_c + (m - \frac{N_F+1}{2})\Delta f$, $m = 1, \ldots, N_F$. Here, we set $f_c = 10$ GHz, $N_F = 7$ and $\Delta f = 100$ MHz. The distance between antennas is $d = c/f_{N_F}$. Fig. 2(a) shows the beam pattern for the first sub-array B_1 and the beam pattern of the last sub-array B_7 when the weights are all set to 1, i.e., $\alpha_{i,m} = 1, \forall\, i, m$. When we set $\alpha_{i,m} = \mathrm{e}^{-j2\pi\frac{f_m}{c}(\frac{N_T-1}{2}-i)d\sin(\frac{\pi}{6})}$, the beam pattern is steering by $\pi/6$ radians (30°), and the beam pattern can be obtained as in Fig. 2(b).

If $D_m(\theta)$ denotes a desired transmission beam pattern, then we can choose an appropriate weighting vector $\boldsymbol{\alpha}_m$ in order to obtain a frequency-wavenumber response and beam pattern with desirable properties. Several approaches for selecting the weighting vector have been investigated in [11]–[13]. For the MIMO frequency diversity radar, we apply these beamforming approaches for each $m = 1, \cdots, N_F$ so that the signal on each carrier frequency can obtain the desired beam pattern. Although we are not discussing the more advanced beamforming techniques for MIMO frequency diversity radar in this work, we demonstrated the beamforming ability of this new radar architecture.

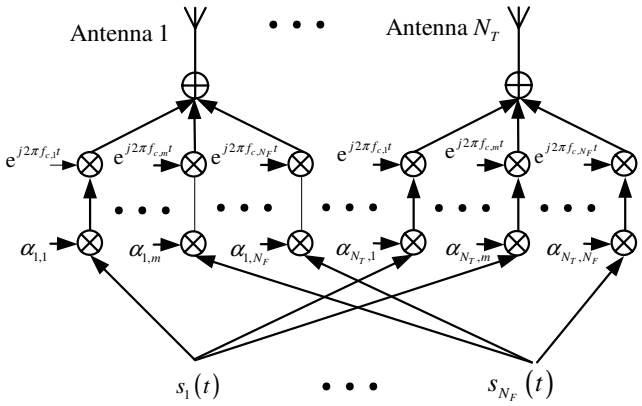

Fig. 1. MIMO radar transmitter design that can exploit frequency diversity.

B. Receiver Architecture

The receiver design of the MIMO radar with frequency diversity is shown in Fig. 3. As we can see, there are N_R receiver antennas and each antenna can receive N_F different carrier frequencies at the same time. At the lth antenna, $l = 1, \ldots, N_R$, the mth carrier frequency f_m is demodulated, and then the demodulated signal is filtered by an appropriate low-pass filter to obtain the baseband signal $r_{l,m}(t)$.

As we assume that the carrier frequency for each transmission signal $s_m(t)$ is widely-separated and in the order of 50 MHz, and that the bandwidth of $s_m(t)$ is in the order of 1 kHz to 10 MHz, then the separation of the signals on different carrier frequencies is feasible using demodulation followed by lowpass filtering. After demodulation and lowpass filtering, the signal $r_{l,m}(t)$, received from the lth antenna and demodulated from the mth carrier frequency, can be given by

$$r_{l,m}(t) = \beta_m s_m(t-\tau)e^{j2\pi f_m\frac{v}{c}t}a_m(l,\theta) + w_{l,m}(t), \qquad (1)$$

where τ is the time-delay introduced by the target reflection, v is the range-rate of the target, and the Doppler frequency of the signal with carrier frequency f_m is given by $\frac{v}{c}f_m$. Note that, as the transmission signal contains multiple widely-separated carrier frequencies, the Doppler frequency shifts are different for each transmission carrier frequency. The lth element of the array steering vector $\mathbf{a}_m(\theta) = [a_m(1,\theta)\ \cdots\ a_m(l,\theta)\ \cdots\ a_m(N_R,\theta)]^{\mathbb{T}}$ is given by $a_m(l,\theta) = \exp(j2\pi(f_m/c)(\frac{N_R-1}{2} - l)\sin(\theta)d)$, and β_m is the target reflection coefficient for the signal on the mth carrier frequency. As we assume that the carrier frequencies are widely-separated, and using the RCS properties for different frequencies as discussed in Section II, we can obtain that $\mathrm{E}\{\beta_{m_1}\beta_{m_2}^*\} = 0$, $\forall\ m_1 \neq m_2$. As the decorrelated RCS corresponds to different carrier frequencies, β_m for different carrier frequencies f_m are also decorrelated. Thus, the signal phase change caused by the signal propagation delay $\exp(j2\pi f_m(v/c)\tau)$ is absorbed in the reflection coefficient β_m and does not appear in the received signal.

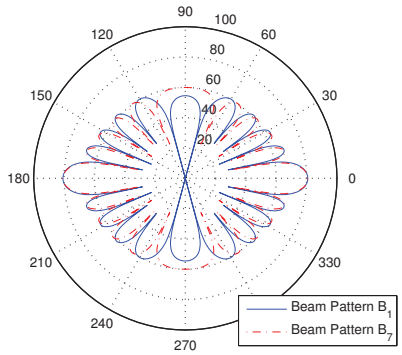

(a)

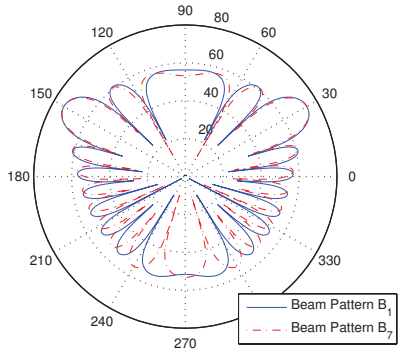

(b)

Fig. 2. (a) Uniform linear array beam pattern B_1 and B_7 (in dB) of sub-arrays with carrier frequency f_1 and f_7, respectively, as a function of direction (in degrees). (b) Same beam pattern after it is steered by 30 degrees.

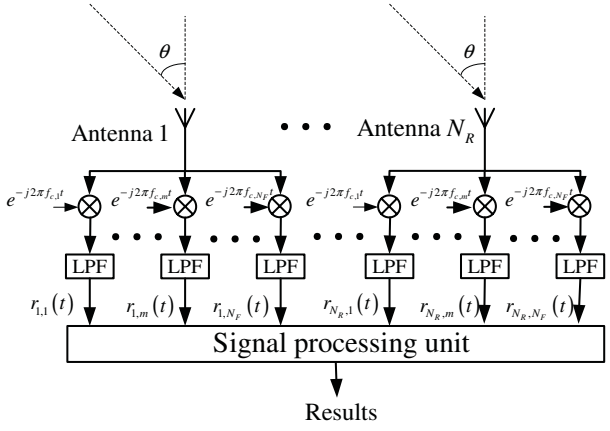

Fig. 3. MIMO radar receiver design that can exploit frequency diversity.

The term $w_{l,m}(t)$ in (1) is additive Gaussian noise. We can reasonably assume that noise terms introduced by by different antennas are independent so that $\mathrm{E}\{w_{l,m}(t)w^*_{l',m'}(t)\} = 0,\ \forall\, l \neq l',\ m \neq m'$. We can also assume that the noise is uncorrelated after demodulation by different carrier frequencies and lowpass filtering because the carrier frequencies are widely separated, i.e., $\{w_{l,m}(t)w^*_{l,m'}(t)\} = 0,\ \forall\ m \neq m'$. Also, noise with the same index (l,m) can be assumed band-limited and hence correlated in time. However, with the assumption that the bandwidth of $s_m(t)$ is much less then the frequency space Δf, after properly sampling using the sampling period interval $T_s \gg 1/\Delta f$, the correlation is very weak, i.e., $\mathrm{E}\{w_{l,m}(pT_s)w^*_{l,m}(qT_s)\} \approx 0$ for $p \neq q$, and σ_w^2 for $p = q$.

The signal processing system in Fig. 3 can also be configured for different purposes, including target detection, direction finding, range-velocity estimation, and tracking. Also, various signal processing algorithms can be employed under this transceiver architecture to improve performance. Next, we discuss one potential performance improvement with this new architecture for target estimation.

IV. Target Estimation Using MIMO Radar with Frequency Diversity

To formulate the target estimation problem for a MIMO radar system with frequency diversity, we first sample the received signal using sampling period T_s, and denote the resulting samples as $r_{l,m}[n] = r_{l,m}(nT_s)$. We consider the noiseless received signal $\mu_{l,m}[n] = s_m(nT_s - \tau)e^{j2\pi f_m(v/c)nT_s}a_m(l,\theta)$ for a simplified notation. We also define the following vectors: $\mathbf{r}_{l,m} = [r_{l,m}[1]\ \cdots\ r_{l,m}[N]\ ]^{\mathbb{T}}$, $\mathbf{r}_m = [\mathbf{r}^{\mathbb{T}}_{1,m}\ \cdots\ \mathbf{r}^{\mathbb{T}}_{N_R,m}]^{\mathbb{T}}$, $\mathbf{r} = [\mathbf{r}^{\mathbb{T}}_1\ \cdots\ \mathbf{r}^{\mathbb{T}}_{N_F}]^{\mathbb{T}}$, $\boldsymbol{\mu}_{l,m} = [\mu_{l,m}[1]\ \cdots\ \mu_{l,m}[N]\ ]^{\mathbb{T}}$, $\mathbf{w}_{l,m} = [w_{l,m}[1]\ \cdots\ w_{l,m}[N]\ ]^{\mathbb{T}}$, and $\boldsymbol{\beta} = [\beta_1\ \cdots\ \beta_{N_F}]^{\mathbb{T}}$.

Using this notation, the probability density function of $\mathbf{r}$ is

$$p(\mathbf{r}|\boldsymbol{\beta},\tau,v,\theta) = 1/(\pi^{NN_RN_F}\det{}^{N_RN_F}(\mathbf{C}_w))$$
$$\times \exp\Big(-\sum_{m=1}^{N_F}\sum_{l=1}^{N_R}(\mathbf{r}_{l,m} - \beta_m\boldsymbol{\mu}_{l,m})^{\mathbb{H}}\mathbf{C}_w^{-1}(\mathbf{r}_{l,m} - \beta_m\boldsymbol{\mu}_{l,m})\Big) \quad (2)$$

where $\mathbf{C}_w = \mathrm{E}\{\mathbf{w}^{\mathbb{H}}_{l,k}\mathbf{w}_{l,k}\}$ is the covariance matrix of $\mathbf{w}_{l,m}$. If we assume white noise, then $\mathbf{C}_w = \sigma_w^2\mathbf{I}_N$, where $\mathbf{I}_N$ is the $N \times N$ identity matrix.

Based on the probability density function in (2), we compute the maximum likelihood estimator (MLE) of the target parameter vector $\boldsymbol{\zeta} = [\beta_1, \cdots, \beta_{N_F}, \theta, \tau, v]^{\mathbb{T}}$ as

$$\widehat{\boldsymbol{\zeta}}_{MLE} = \max_{\beta_1,\cdots,\beta_{N_F},\theta,\tau,v} p(\mathbf{r}|\beta_1, \cdots, \beta_{N_F}, \theta, \tau, v).$$

If we treat the reflection coefficients $\beta_1, \cdots, \beta_{N_F}$ as nuisance parameters, and we define $\boldsymbol{\phi} = [\theta, \tau, v]^{\mathbb{T}}$, then with the white noise assumption $\mathbf{C}_w = \sigma_w^2\mathbf{I}_N$, then the MLE of $\boldsymbol{\phi}$ is

$$\widehat{\boldsymbol{\phi}}_{MLE} = \max_{\theta,\tau,v} \frac{1}{\sigma_w^2}\sum_{m=1}^{N_F}\frac{\Big|\sum_{l=1}^{N_R}\mathbf{r}^{\mathbb{H}}_{l,m}\boldsymbol{\mu}_{l,m}\Big|^2}{\sum_{l=1}^{N_R}\boldsymbol{\mu}^{\mathbb{H}}_{l,m}\boldsymbol{\mu}_{l,m}}. \quad (3)$$

The MLE performance can be characterized by the CRLB on the estimation covariance when the SNR is large or when large

data records are available. From (3), we can see that the MLE of ϕ can be obtained by combining the MLE of each sub-array. Thus, we can also use the CRLB results derived in [14] for estimating range, velocity, and direction with an active array.

In order to find the CRLB of $\boldsymbol{\phi} = [\theta \ \tau \ v]^{\mathbb{T}}$, we first denote $\boldsymbol{\eta} = [\tau \ v]^{\mathbb{T}}$. For the mth sub-array, we denote the signal vectors as a function of $\boldsymbol{\eta} = [\tau \ v]^{\mathbb{T}}$ as $\mathbf{s}_m(\boldsymbol{\eta}) = [s_m(T_s - \tau)e^{j2\pi f_m(v/c)T_s} \ldots s_m(NT_s - \tau)e^{j2\pi f_m(v/c)NT_s}]^{\mathbb{T}}$. As a result, we can obtain the following intermediate results for the mth sub-array

$$\text{CRLB}^m_{\theta\theta} = \sigma_w^2 \left[\mathcal{I}^m_{\theta\theta} - \frac{\text{Re}\{\mathbf{P}^m_{\theta\beta}\mathbf{P}^{m\mathbb{H}}_{\theta\beta}\}}{2\mathbf{s}^{\mathbb{H}}_m(\boldsymbol{\eta})\mathbf{s}_m(\boldsymbol{\eta})\mathbf{a}^{\mathbb{H}}_m(\theta)\mathbf{a}_m(\theta)} \right]^{-1} \quad (4)$$

$$\text{CRLB}^m_{\boldsymbol{\eta}\boldsymbol{\eta}} = \sigma_w^2 \left[\mathcal{I}^m_{\boldsymbol{\eta}\boldsymbol{\eta}} - \frac{\text{Re}\{\mathbf{P}^m_{\boldsymbol{\eta}\beta}\mathbf{P}^{m\mathbb{H}}_{\boldsymbol{\eta}\beta}\}}{2\mathbf{s}^{\mathbb{H}}_m(\boldsymbol{\eta})\mathbf{s}_m(\boldsymbol{\eta})\mathbf{a}^{\mathbb{H}}_m(\theta)\mathbf{a}_m(\theta)} \right]^{-1} \quad (5)$$

$$\text{CRLB}^m_{\theta\boldsymbol{\eta}} = \mathbf{0} \quad (6)$$

where

$$\mathcal{I}^m_{\theta\theta} = 2\,|\beta_m|^2 \mathbf{s}^{\mathbb{H}}_m(\boldsymbol{\eta})\mathbf{s}_m(\boldsymbol{\eta}) \text{Re}\{\frac{\partial \mathbf{a}^{\mathbb{H}}_m(\theta)}{\partial\theta}\frac{\partial \mathbf{a}_m(\theta)}{\partial\theta}\} \quad (7)$$

$$\mathbf{P}^m_{\theta\beta} = 2\,\mathbf{s}^{\mathbb{H}}_m(\boldsymbol{\eta})\mathbf{s}_m(\boldsymbol{\eta})\beta^{\mathbb{H}}_m \frac{\partial \mathbf{a}^{\mathbb{H}}_m(\theta)}{\partial\theta}\mathbf{a}_m(\theta) \quad (8)$$

$$\mathcal{I}^m_{\boldsymbol{\eta}\boldsymbol{\eta}} = 2\,|\beta_m|^2 \frac{\partial \mathbf{s}^{\mathbb{H}}_m(\boldsymbol{\eta})}{\partial\boldsymbol{\eta}}\frac{\partial \mathbf{s}_m(\boldsymbol{\eta})}{\partial\boldsymbol{\eta}} \text{Re}\{\mathbf{a}^{\mathbb{H}}_m(\theta)\mathbf{a}_m(\theta)\} \quad (9)$$

$$\mathbf{P}^m_{\boldsymbol{\eta}\beta} = 2\,\beta^{\mathbb{H}}_m \mathbf{a}^{\mathbb{H}}_m(\theta)\mathbf{a}_m(\theta)\frac{\partial \mathbf{s}^{\mathbb{H}}_m(\boldsymbol{\eta})}{\partial\boldsymbol{\eta}}\mathbf{s}_m(\boldsymbol{\eta}). \quad (10)$$

If we substitute (7)-(10) into (4) and (5), the CRLB for DOA and range-Doppler estimation can be obtained as

$$\text{CRLB}_{\theta\theta} = \left[\sum_{m=1}^{N_F} 2|\beta_m|^2 \frac{E_m}{\sigma_w^2} \left(\frac{\partial}{\partial\theta}\mathbf{a}^{\mathbb{H}}_m(\theta)\frac{\partial}{\partial\theta}\mathbf{a}_m(\theta) - \frac{\frac{\partial}{\partial\theta}\mathbf{a}^{\mathbb{H}}_m(\theta)\,\mathbf{a}^{\mathbb{H}}_m(\theta)\,\mathbf{a}_m(\theta)\,\frac{\partial}{\partial\theta}\mathbf{a}_m(\theta)}{\mathbf{a}^{\mathbb{H}}_m(\theta)\mathbf{a}_m(\theta)} \right) \right]^{-1} \quad (11)$$

$$\text{CRLB}_{\boldsymbol{\eta}\boldsymbol{\eta}} = \left[\sum_{m=1}^{N_F} 2|\beta_m|^2 N_R \frac{1}{\sigma_w^2} \left(\frac{\partial}{\partial\boldsymbol{\eta}}\mathbf{s}^{\mathbb{H}}_m(\boldsymbol{\eta})\frac{\partial}{\partial\boldsymbol{\eta}}\mathbf{s}_m(\boldsymbol{\eta}) - \frac{1}{E_m}\frac{\partial}{\partial\boldsymbol{\eta}}\mathbf{s}^{\mathbb{H}}_m(\boldsymbol{\eta})\,\mathbf{s}_m(\boldsymbol{\eta})\,\mathbf{s}^{\mathbb{H}}_m(\boldsymbol{\eta})\frac{\partial}{\partial\boldsymbol{\eta}}\mathbf{s}_m(\boldsymbol{\eta}) \right) \right]^{-1} \quad (12)$$

$$\text{CRLB}_{\theta\boldsymbol{\eta}} = \mathbf{0}.$$

V. Numerical Examples

We consider the $\text{CRLB}_{\boldsymbol{\eta}\boldsymbol{\eta}}$ as an example to illustrate how frequency diversity can improve estimation performance. We start by making some assumptions to simplify (12). We first assume that all sub-arrays use the same waveform, $s_m(t) = s(t)$, and thus have the same energy E_s. We also assume that $\mathbf{a}^{\mathbb{H}}_m(\theta)\mathbf{a}_m(\theta) = N_R$ is the array gain. The CRLB of $\boldsymbol{\eta} = [\tau \ v]^{\mathbb{T}}$ thus simplifies to

$$\text{CRLB}_{\boldsymbol{\eta}\boldsymbol{\eta}} = \left[\sum_{m=1}^{N_F} 2|\beta_m|^2 N_R \frac{E_s}{\sigma_w^2}\mathcal{I}^{\boldsymbol{\eta}} \right]^{-1}, \quad (13)$$

where

$$\mathcal{I}^{\boldsymbol{\eta}} = \frac{\partial}{\partial\boldsymbol{\eta}}\mathbf{s}^{\mathbb{H}}(\boldsymbol{\eta})\frac{\partial}{\partial\boldsymbol{\eta}}\mathbf{s}(\boldsymbol{\eta}) - \frac{1}{E_s}\frac{\partial}{\partial\boldsymbol{\eta}}\mathbf{s}^{\mathbb{H}}(\boldsymbol{\eta})\,\mathbf{s}(\boldsymbol{\eta})\,\mathbf{s}^{\mathbb{H}}(\boldsymbol{\eta})\frac{\partial}{\partial\boldsymbol{\eta}}\mathbf{s}(\boldsymbol{\eta}).$$

In (13), if we treat $2N_R\frac{E_s}{\sigma_w^2}\mathcal{I}^{\boldsymbol{\eta}}$ as a constant, then the CRLB is actually a function of $\sum_{m=1}^{N_F}|\beta_m|^2$. For example, without frequency diversity, (or, equivalently, if $N_F = 1$), if the target is slowly fluctuating, the reflection coefficient β will vary very slowly, and if the carrier frequency has a very weak reflection from the target, the detection performance will be greatly reduced. However, with frequency diversity, the combination of all the reflection coefficients $\sum_{m=1}^{N_F}|\beta_m|^2$ will be almost constant as the target could react differently for each frequency. The effect of frequency diversity is demonstrated in Fig. 4 that shows the mean-squared error (MSE) performance of a phased array radar whose carrier frequency is such that there is a 3 dB energy loss. Fig. 4 also shows the performance of a MIMO radar with the same total transmission energy that uses frequency diversity to obtain better MSE performance.

For a fast fluctuation target, β_m varies fast and thus the estimation is poor. However, with frequency diversity, the fluctuation can be greatly reduced, and an improved estimation performance can be achieved. This scenario is demonstrated in Fig. 5 that shows the estimation mean value and MSE performance (showed as vertical bars in the figure) of a phased array radar with a single carrier frequency, and the performance of a MIMO radar with the same total transmission energy. Due to the fast fluctuation, the phased array radar performance varies dramatically. Thus, in realistic applications, the target fluctuation will greatly affect the estimation performance. However, the MIMO radar with frequency diversity can greatly reduce errors introduced by target fluctuations.

VI. Conclusion

We proposed a MIMO radar system with frequency diversity by combining a radar array with frequency-division multiplexing. This new system is important in reducing target fluctuations, and it was also shown to incorporate beamforming for designing a transmission beam pattern. We investigated the corresponding estimation algorithm with frequency diversity, and we derived the estimation CRLB. Using numerical results, we showed the improved performance obtained by a MIMO frequency diversity radar system with fast fluctuating targets.

References

[1] E. Fishler, A. Haimovich, R. Blum, L. J. Cimini, Jr., D. Chizhik, and R. Valenzuela, "Spatial diversity in radars-models and detection performance," *IEEE Transactions on Signal Processing*, vol. 54, no. 3, pp. 823–838, 2006.

[2] K. W. Forsythe, D. W. Bliss, and G. S. Fawcett, "Multiple-input multiple-output (MIMO) radar: performance issues," in *Proceedings of Asilomar Conference on Signals, Systems and Computers*, vol. 1, 2004, pp. 310–315.

[3] N. H. Lehmann, A. M. Haimovich, R. S. Blum, and L. Cimini, "High resolution capabilities of MIMO radar," in *Proceedings of Asilomar Conference on Signals, Systems and Computers*, 2006, pp. 25–30.

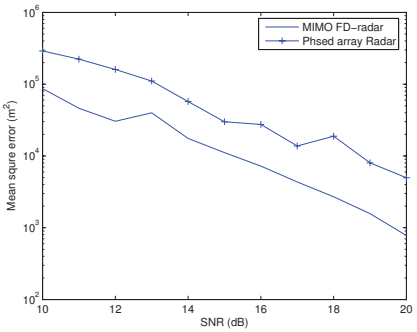

(a)

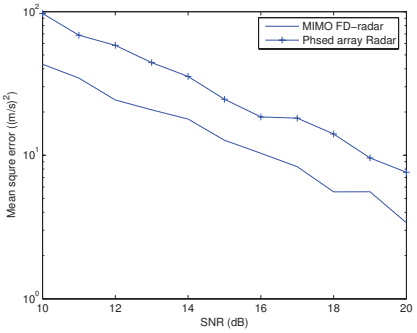

(b)

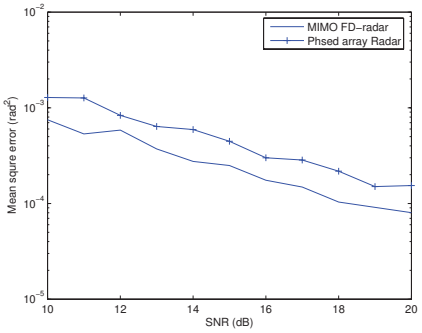

(c)

Fig. 4. Estimation MSE of (a) range, (b) range-rate, and (c) DOA estimation of a slow-fluctuating target.

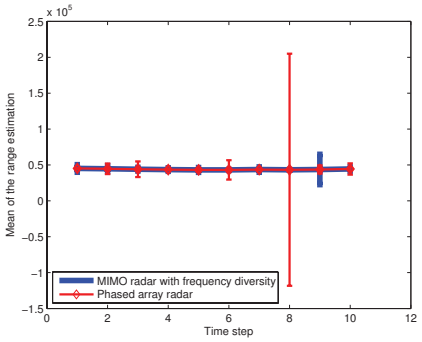

(a)

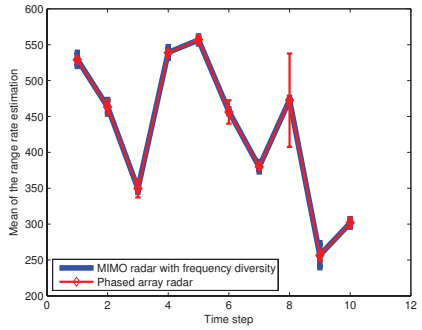

(b)

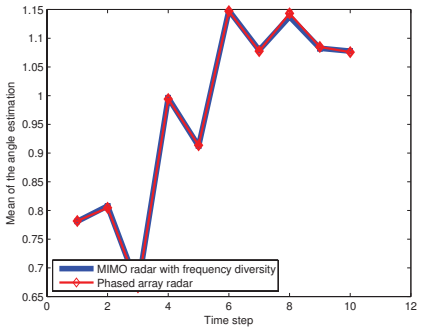

(c)

Fig. 5. Estimation MSE of (a) range, (b) range-rate, and (c) DOA estimation of a fast-fluctuating target.

[4] A. M. Haimovich, R. S. Blum, and L. J. Cimini, "MIMO radar with widely separated antennas," *IEEE Signal Processing Magazine*, vol. 25, no. 1, pp. 116–129, 2008.

[5] J. Li and P. Stoica, "MIMO radar with colocated antennas," *IEEE Signal Processing Magazine*, vol. 24, no. 5, pp. 106–114, 2007.

[6] F. E. Nathanson, J. P. Reilly, and M. N. Cohen, *Radar Design Principles: Signal Processing and the Environment*, 2nd ed. New York: McGraw-Hill, Inc., 1990.

[7] M. A. Richards, *Fundamentals of Radar Signal Processing*. New York: McGraw-Hill, Inc., 2005.

[8] V. Vannicola, "Detection of slow fluctuating targets with frequency diversity channels," *IEEE Transactions on Aerospace and Electronic Systems*, vol. AES-10, pp. 43–52, Jan. 1974.

[9] V. Ravenni and G. Pizziol, "Frequency diversity radar system: Design, analysis and performances," in *Proceedings of 3rd European Radar Conference*, 2006, pp. 221 – 224.

[10] V. Ravenni, "Performance evaluations of frequency diversity radar system," in *Proceedings of European Microwave Conference*, Munich, 2007, pp. 1715 – 1718.

[11] H. L. Van Trees, *Optimum Array Processing, Part IV of Detection, Estimation, and Modulation Theory*. New York: Wiley-Interscience, 2002.

[12] P. Stoica, J. Li, and Y. Xie, "On probing signal design for MIMO radar," *IEEE Transactions on Signal Processing*, vol. 55, no. 8, pp. 4151–4161, 2007.

[13] L. Xu, J. Li, and P. Stoica, "Adaptive techniques for MIMO radar," in *Proceedings of IEEE Sensor Array and Multichannel Signal Processing Workshop*, 2006, pp. 258–262.

[14] A. Dogandzic and A. Nehorai, "Cramér-Rao bounds for estimating range, velocity, and direction with a sensor array," *IEEE Transactions on Signal Processing*, vol. 49, pp. 1122 – 1137, 2001.